Interference effects between 4*s* photoionization and resonant Auger-decay channels at inner-shell $3d^9 4p^5 nln'l'$ double excitations in Kr

S. Alitalo, T. Matila, H. Aksela, A. Kivimäki, M. Jurvansuu, and S. Aksela
Department of Physical Sciences, University of Oulu, P.O. Box 3000, FIN-90014 University of Oulu, Finland
(Received 21 March 2000; published 15 August 2000)

Changes in Kr 4*s* photoelectron satellite intensities caused by interference with the Auger decay of inner-shell doubly excited $3d^9 4p^5 nln'l'$ states are studied by high-resolution experiment and one-step calculations. The calculations predict pronounced interference effects in the relative intensity of the most intense satellite line $4p^4(^1D)4d(^2S_{1/2})$ as a function of photon energy, in good agreement with experiment.

PACS number(s): 32.80.Hd, 32.80.Fb

I. INTRODUCTION

The possibility of tuning photon energy continuously using synchrotron radiation offers an effective tool to study various photon-energy-dependent phenomena in atomic and molecular photoionization. It has also become increasingly feasible to determine single and multiple excitation and ionization cross sections for various subshells of atoms and molecules (see, e.g., Refs. [1–13], and references therein). For krypton, 4*p*, 4*s*, and 3*d* partial photoionization cross sections were widely studied by both experiment and theory [6–8]. Above the 3*d* threshold the 3*d* ionization gives the largest contribution to the total cross section (~65% at around 120 eV), the rest being divided between the 4*p* and 4*s* cross sections (~5% and ~30%, respectively, at 120 eV) [6].

At certain photon energies above a core ionization threshold, a core electron and an additional outer-shell electron can both be resonantly excited to unoccupied Rydberg orbitals, i.e., a neutral doubly excited state is created (see, e.g., Refs. [14,15], and references therein). The doubly excited states above the 3*d* threshold of Kr were studied by Hayaishi *et al.* [16] by measuring a total ion yield spectrum which corresponds to the photoabsorption spectrum. Strengths of the double excitations can be estimated from their spectrum to be less than 5% of the strongest one-electron excitation, $3d_{5/2} \rightarrow 5p$.

Analogously to singly excited states (e.g., $3d^9 np$), doubly excited states decay prominently via resonant Auger transitions, where the initially excited electrons may or may not take part in the filling of the holes. In a single-participator process one of the excited electrons participates actively while the other remains as a spectator (e.g., $3d^9 4p^5 nln'l' \rightarrow 4p^4 nl$). Partial ion yield spectra recorded in the photon energy region of two-electron excitations in Kr [8] did not show any visible production of singly charged ions, indicating that the single participator channel does not play any prominent role. This is in agreement with the predictions for similar processes in Xe [14], where the double-participator channel was seen to be the dominating recombination channel. The single-participator channel was, however, found to result in clear intensity variations of several Xe $5p^4 nl$ states [14].

Kr $4p^4 nl$ states can also be reached via direct 4*s* and 4*p* photoionization as correlation and shakeup satellites. The former are due to strong interaction between the close-lying states of the $4s^{-1}$ and $4p^4 ns,nd$ configurations while the latter arise from the $4p \rightarrow np$ shakeup transitions accompanying 4*p* ionization [17]. For instance, the intensity of the strongest photoelectron satellite line $4p^4(^1D)4d(^2S_{1/2})$ was observed to be 17.1% relative to the 4*s* main line at photon energy $h\nu = 88$ eV [18].

Since the single-participator resonant Auger final states can also be reached via direct photoionization, interference of the two channels becomes possible. This effect is expected to be very important at doubly excited resonances, as the two channels are of the same order of magnitude.

II. CALCULATIONS

The variation of photoelectron satellite intensity with respect to excitation energy can be calculated following the time-independent scattering formalism (see Ref. [1], and references therein). Following Ref. [1], the scattering amplitude becomes

$$A_F = \langle [f,f']\phi\varepsilon | V | o \rangle + \sum_{[i,i']} \int d\tau \int d\tau' \times \frac{\langle [f,f']\phi\varepsilon | H - E_F | [i,i']\tau\tau' \rangle \langle [i,i']\tau\tau' | V | o \rangle}{E_F - E_{\tau\tau'} + i\Gamma_{[i,i']}/2}. \quad (1)$$

The first term represents the amplitude for a direct ionization process whereas the second term is due to the contribution following from a double excitation. The notations in Eq. (1) follow Armen *et al.* [1], with small modifications. $[i,i']$ represents the intermediate two-hole state, $E_{\tau\tau'} = E_0 + I_{[i,i']} + \tau + \tau'$ its total energy, and $\Gamma_{[i,i']}$ its total width. The integrations over τ and τ' include implicit summations over bound states.

In order to utilize Eq. (1), we have made further simplifications by factorizing the photon-electron interaction matrix elements in the second term of Eq. (1) as follows:

$$\sum_{\tau,\tau'}\langle[i,i']\tau\tau'|V|o\rangle \approx \sum_{n,n'}\langle[3d,4p]np\ n'p|V|o\rangle + \sum_{m,m'}\langle[3d,4p]ml\ m'd,(l=s,d)|V|o\rangle$$

$$\approx \sum_{n,n'} d_n c_n((3d^9np)^1P,(4p^5n'p)^{2S'+1}L')\langle 4p_o|n'p\rangle\delta_{0S'}\delta_{0L'}$$

$$+ \sum_{m,m'} d_{m,l}c_{m,l}[(3d^9ml,(l=s,d))^1P,(3d^9m'd)^{2S'+1}L']\langle 3d_o|m'd\rangle\delta_{0S'}\delta_{0L'}$$

$$\approx \sum_{n} d_n[c_n((3d^9np)^1P,4p^6)+c_n((3d^9np)^1P,(4p^55p)^1S)\langle 4p_o|5p\rangle]$$

$$+ \sum_{m} d_{m,l}c_{m,l}[(3d^9ml,(l=s,d))^1P,(3d^94d)^1S]\langle 3d_o|4d\rangle. \quad (2)$$

The matrix elements in the first term of Eq. (1), related to photoelectron satellites, are given by

$$\langle[f,f']\phi\varepsilon|V|o\rangle = d_\varepsilon c(4s^{-1}\varepsilon p\ ^1P). \quad (3)$$

In Eqs. (2) and (3) the subscript o indicates the ground-state wave function, and c's are the mixing coefficients of the LS basis states in the intermediate coupling including configuration interaction (CI). $d_n \propto \varepsilon_{ph}\langle 3d||\mathbf{r}||np\rangle$, $d_{m,l} \propto \varepsilon_{ph}\langle 4p||\mathbf{r}||ml,(l=s,d)\rangle$ and $d_\varepsilon \propto \varepsilon_{ph}\langle 4s||\mathbf{r}||\varepsilon p\rangle$ are factors including the reduced dipole matrix elements and the photon energy dependence. $\langle 4p_o|5p\rangle$ and $\langle 3d_o|4d\rangle$ are overlap integrals related to the shake processes.

The first term in Eq. (2) with $n'p=4p$ can be interpreted by means of electron correlation. It is the portion of a singly excited state in a doubly excited state. In our calculations we have taken into account the terms with $n=5$, 6, 7, 8, and 9 in summation. The term in Eq. (2) where $n'p=5p$ can be interpreted as a $3d\rightarrow np$ dipole transition accompanied by a simultaneous $4p\rightarrow 5p$ monopole shake-up. In addition we have accounted only for the $n=5$ and 6 terms in summation. The last term in Eq. (2) can be interpreted as a $4p \rightarrow md,ms$ dipole transition accompanied by a simultaneous $3d\rightarrow 4d$ shake-up. Only cases $md=4d$ and $ms=5s$ were considered. We have neglected the possible portions of singly excited $4p^{-1}(md,ms)$ states in the doubly excited state. Equation (3) can be interpreted as electron correlation: photoionization leading to $4p^{-2}nd,ns$ states may occur only via CI with the $4s^{-1}$ states.

In the calculations of Auger decay matrix elements $\langle[f,f']\phi\varepsilon|H-E_F|[i,i']\tau\tau'\rangle$ in Eq. (1), some further simplifications were made. $((4p^4\ ^1D)4d)^2S_{1/2}$, together with $4s^{-1}$ are the leading configurations for the main $4s$ photoelectron line and for the strongest photoelectron satellite line. Thus we reduced the Auger amplitudes needed in the one-step calculation (for the peak under consideration, see below) to include only one $\langle[f,f']\phi\varepsilon|$ state, namely, $[[((4p^4\ ^1D)4d)^2S_{1/2}]\epsilon p]^1P_1$, which is expected to be responsible for the strongest interference effects.

In the calculations our basis set for the resonant states was restricted to include the LSJ states from the $3d^94p^5[5s^2,4d^2,5p^2,5p^1(6p^1,7p^1,8p^1,9p^1),6p^1(7p^1,8p^1,9p^1),4d^15s^1]$ and $3d^94p^6(6p^1,7p^1,8p^1,9p^1)$ configurations, and for the final state it included LSJ states only from the $4p^44d\epsilon p$ configuration. For direct photoionization we performed a small CI calculation, including the LSJ states from the $4s^14p^6$ and $4s^24p^4(4d-7d,5s-8s)$ configurations.

The dipole and Auger decay matrix elements, shakeup integrals, and eigenfunctions for the resonant and final states were calculated using the Hartree-Fock method with relativistic corrections (HFR), which means that the effects of mass velocity and Darwin terms on radial wave functions were taken into account spin independently using the Cowan-Griffin operator [20]. Spin-orbit interaction was added as a pertubation by using the Blume-Watson method [21]. The dipole and shake matrix elements were calculated using the ground-state wave functions for the initial state, the relaxed wave functions from the $3d^94p^5nln'l'$ type configurations for the resonant state, and those from $4s^{-1}\varepsilon p$ configurations with proper photoelectron energy for the direct photoionization. The HFR continuum orbitals used in the calculations of Auger-decay matrix elements were generated in the configuration-average potentials of the $4p^4(^1D)4d$ electron configuration. Its energy was chosen to be the difference between the configuration-average energies of the $3d^94s^24p^55p^2$ and $4p^4(^1D)4d$ electron configurations. All calculations were performed using Cowan's code [19]. The relative intensity of the $4p^4(^1D)4d(^2S_{1/2})$ line is shown in Fig. 1, calculated in different ways. Figure 1(a) refers to a calculation where the first term of Eq. (2), the CI with a single excited state, was accounted for (labeled by CI in the figure caption and below). Figures 1(b) and 1(c) refer to calculations accounting only for the second and third terms of Eq. (2), respectively. (These calculations are called the $3d$ shake and $4p$ shake.) In Fig. 1(d) the total effect of these three terms is presented (Total 1). Next the effects of double excitations on the intensity of the main $4s$ photoelectron line were included. The result (Total 2) is shown in Fig. 1(e).

III. EXPERIMENT AND DISCUSSION

The experiments were performed on the new undulator beamline I411 at the 1.5-GeV MAX–II storage ring at Lund,

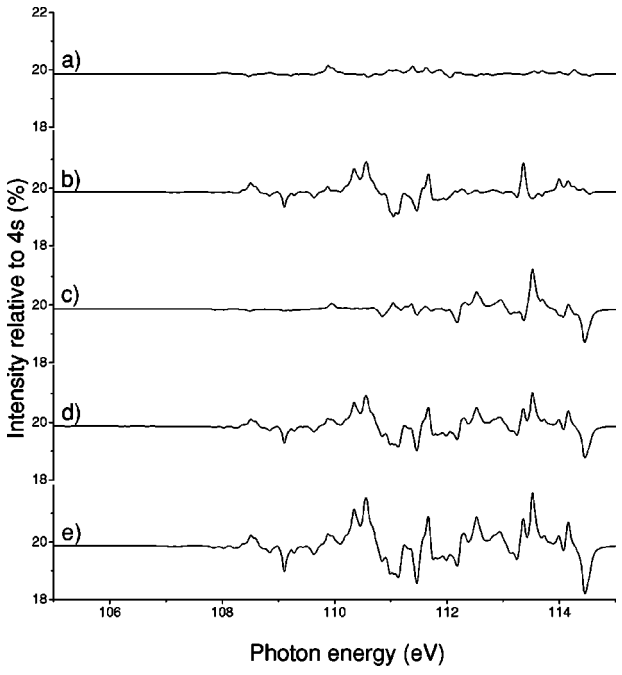

FIG. 1. Calculated intensity variations of the $4p^4(^1D)4d(^2S_{1/2})$ line as a function of photon energy. Calculation (a) refers to calculation labeled by CI in the text, (b) and (c) to $3d$ and $4p$ shake calculations, respectively, (d) to the calculation labeled by Total 1 and (e) by Total 2.

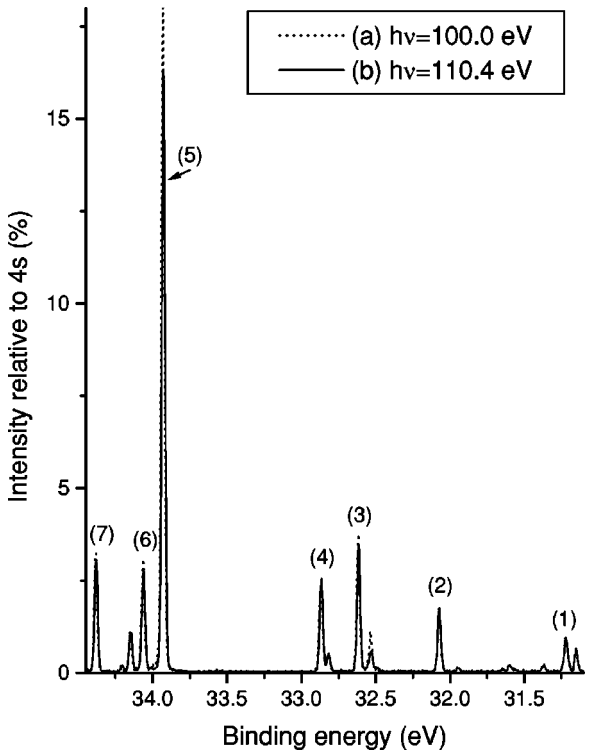

FIG. 2. The $4s$ photoelectron satellite spectra taken at (a) 100.0-eV and (b) 110.4-eV photon energies. Line 1 corresponds to the final state $4p^4(^3P)5p(^2P_{1/2})$; line 2 to state $4p^4(^1S)5s(^2S_{1/2})$; line 3 to states $4p^4(^1D)5p(^2P_{3/2})$ and $4p^4(^1D)4d(^2D_{3/2})$; line 4 to states $4p^4(^1D)4d(^2P_{1/2})$, $4p^4(^1D)5p(^2D_{3/2})$, $4p^4(^1D)5p(^2P_{1/2})$, and $4p^4(^1D)5p(^2D_{5/2})$; line 5 to the state $4p^4(^1D)4d(^2S_{1/2})$; line 6 to the states $4p^4(^3P)6s(^4P_{1/2})$, $4p^4(^3P)6s(^2P_{3/2})$, and $4p^4(^3P)5d(^4D_{3/2})$, and line 7 to the state $4p^4(^1S)6s(^2S_{1/2})$.

Sweden. Radiation in the photon energy range from 50 eV to well above 1000 eV is monochromatized by a modified SX-700 plane-grating monochromator [22]. The resonant Auger spectra of Kr were excited with very high photon resolution of $\sim$10 meV. Ejected electrons were recorded with a rotatable SES-200 hemispherical analyzer [23], using a 10-eV pass energy, which corresponds to a kinetic energy resolution of about 20 meV. The $4s$ photoelectron satellite spectra were measured at photon energies 100–120 eV in a binding-energy region of 36.9–26.6 eV. The binding-energy scale was calibrated using the energy values of Minnhagen *et al.* [24].

Two spectra covering the binding energy region of 34.45–31.10 eV, taken at $h\nu=100.0$ (a) and 110.4 eV (b) photon energies, are shown in Fig. 2. Spectra (a) and (b) were recorded at photon energies below and at the double-excitation resonances, respectively. The assignments of the most intense lines are given in the caption of Fig. 2. The assignment of line 1 is the same as in Refs. [24,25], and also like that of line 2, in which, according to our calculations, the $4p^4(^1S)5s(^2S_{1/2})$ character plays a dominant role. Two final states of different parity overlap in the energy in the case of line 3 [24,25], but as CI is allowed within the $J=1/2$ states only, the $4p^4(^1D)4d(^2D_{3/2})$ state cannot be populated as a correlation satellite of the $4s$ photoelectron line. We thus suppose that the variation of line 3 displays the behavior of the $4p^4(^1D)5p(^2P_{3/2})$ state. In the case of line 4 there are several final states close by in energy [24,25]; hence we omit it in our future considerations. The strongest photoelectron satellite line 5 is according to our calculations a complex mixture of the $4p^4(^1D)nd(^2S_{1/2})$, $n=4-7$, and $4s^{-1}(^2S_{1/2})$ states. With a limited basis set the contribution of higher states is overestimated, however, and therefore we do not argue with the label $4p^4(^1D)4d(^2S_{1/2})$ given in Ref. [24], whereas the label $4p^4(^3P)5d(^4P_{1/2})$ in Ref. [25] may not correspond to the largest eigenvector contribution in this heavily mixed state. The states $4p^4(^3P)6s(^4P_{1/2})$, $4p^4(^3P)6s(^2P_{3/2})$, and $4p^4(^3P)5d(^4D_{3/2})$ overlap at the position of line 6 [24,25]. As only the $J=1/2$ states are populated via CI with the $4s^{-1}$ state, we think that the $4p^4(^3P)6s(^4P_{1/2})$ assignment is relevant for this line in the photoelectron spectrum, but one should not forget the mixing with other states with $J=1/2$. The assignment of line 7 as $4p^4(^1S)6s(^2S_{1/2})$ was taken from Moore [25]. According to our calculations this state is not substantially mixed. Therefore, the label $4p^4(^3P)5d(^4P_{1/2})$ given in Ref. [24] for this state is somewhat suprising. The other strong photoelectron satellite line at 36.47-eV binding energy, is, according to our calculations, heavily mixed from the $4p^4(^1D)nd(^2S_{1/2})$, $n=4$ and 5, $4p^4(^2S)4s(^2S_{1/2})$, and $4p^4(^3P)5d(^2P_{1/2})$ states. In accordance with Ref. [18], we label this line as $4p^4(^1D)5d(^2S_{1/2})$, even though a single-configuration assignment should not be taken literally. The label $4p^4(^3P)8s(^4P_{3/2})$ given in Ref. [24] does not fit well to a photoelectron satellite created via CI.

The intensities of the satellites were extracted from the fit

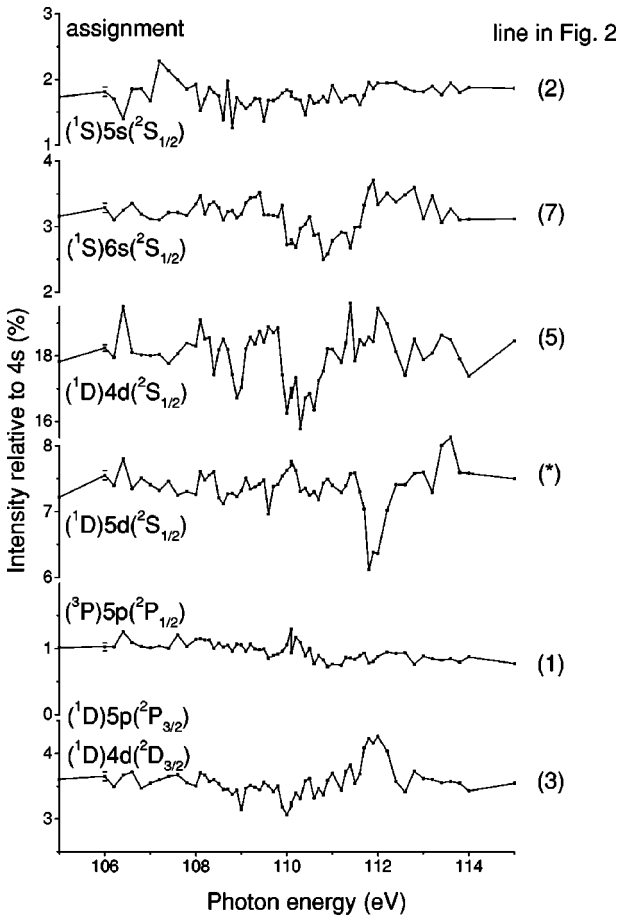

FIG. 3. (a) Experimental intensity variations of lines 1, 2, 3, 5, and 7 of Fig. 2 as a function of photon energy. The asterisk corresponds to line $4p^4(^1D)5d(^2S_{1/2})$, not shown in Fig. 2; it is located at a binding energy of 36.47 eV. Estimated inaccuracies are shown at 106.0 eV.

of the spectra, and determined relative to the $4s$ photoelectron line intensity. Different fits performed for the spectra gave slightly different results which were used to determine the uncertainly due to data treatment. In addition, the statistical error is estimated to be of the same order. Intensity variations of some selected satellites are shown in more detail in Fig. 3 as a function of photon energy. No clear changes were detected below and above the displayed photon energy range.

Clear resonances can be observed in Fig. 3. The $4p^45s$ lines already show strong resonances at photon energies of 106–109 eV [see the $4p^4(^1S)5s(^2S_{1/2})$ line in Fig. 3, which corresponds to line 2 in Fig. 2], whereas the $4p^4(^1S)6s(^2S_{1/2})$ (line 7 in Fig. 2) shows notable resonances between 108 and 113 eV. Also for the $4p^4nd$ lines, the $4p^4(^1D)4d(^2S_{1/2})$ starts to resonate before the $4p^4(^1D)5d(^2S_{1/2})$ line. Conversely, the $4p^4np$ lines do not show such strong resonances, which was also observed in the behavior of the $5p^4np$ satellites in Xe [14]. Population of the $4p^4(^3P)5p(^2P_{1/2})$ state via direct photoionization is weak, and the detection of the interference becomes difficult. Line 3 of Fig. 2, which we assigned to be mainly of $4p^4(^1D)5p(^2P_{3/2})$ character, shows clear resonances around 112 eV.

Relative intensity variations of the $4p^4ns$ lines are somewhat stronger than those of the $4p^4nd$ lines. The intensity variation of the $4p^4(^1D)5d(^2S_{1/2})$ line is also clearly stronger than that of the $4p^4(^1D)4d(^2S_{1/2})$ line. The energy region and strength of the observed intensity variations of satellites, if explained by single-participator resonant Auger decay from the $3d^94p^5nln'l'$ doubly excited states, allow us to tentatively assign the character of one of the excited electrons to $5s$ and $6s$ or $4d$ and $5d$. At excitation energies of 106–109 eV, the $5s$ seems to be involved, whereas $6s$ and $4d$ lines contribute above 108 eV, and $5d$ and $5p$ somewhat later. This experimental argumentation is well in line with the calculated energy regions of the $3d^94p^5nln'l'$ states.

As the intensities of the photoelectron lines are given relative to the $4s$ line they do not correspond to the partial cross section. In principle they also contain the variations of the reference line, the $4s$ main line. However, the calculations indicate that the interference effects of the $4s$ line follow those of the $4p^4(^1D)4d(^2S_{1/2})$ satellite line, but with a different sign. This gives very similar variations for the satellite, if one compares its relative intensities in the cases where the effect of double excitations on the $4s$ line is taken into account [Total 2 in Fig. 1(e)], and where it is not taken into account [Total 1 in Fig. 1(d)]. The variations have slightly weaker amplitudes in the latter.

A comparison between the experimental (Fig. 3) and calculated [Fig. 1(e)] profiles shows that the calculations reproduce the general behavior of resonances seen in experiment, but finer details are not reproduced. Strong changes around 110 eV in experiment are also shown in calculations, slightly shifted to higher energies only. At higher photon energies the variations are clearly overestimated by calculations. A clear peak in the relative intensity at 106.4 eV is not predicted by theory. CI is weak [Fig. 1(a)], and a $3d$ shake [Fig. 1(b)] starts to affect the $4p^4(^1D)4d(^2S_{1/2})$ intensity only above 108 eV, and the $4p$ shake [Fig. 1(c)] even later, which indicates that the peak at 106.4 eV is not created by the interplay of the photoelectron satellite and the $3d$ and the $4p$ shake channels.

The remaining discrepancies between experiment and theory may also be related to the approximations explained in Sec. II, Eqs. (2) and (3), or to the simplifications in actual calculations. According to our test calculations, CI between doubly excited and singly excited $4p^5nd,ns$ and $4s^1np$ states may also be of importance. Thus the dipole excitations to singly excited states may also contribute to the population of doubly excited states. A complete study, in which such effects could be accounted for, would include configurations with higher ns, np, nd, and nf and possibly continuum orbitals, and furthermore configurations of type $4(p,s)^{-3}nln'l'n''l''$, making such calculations impossible to perform with the present method. We are also skeptical about the quality of calculations at photon energies above 113 eV. A further increment of the basis set seems to cause a significant intensity redistribution in this area. This is most probably the reason for the disagreement between experi-

ment and calculations at about 114 eV. In contrast, for photon energies of about 107–112 eV the calculation seems to be quite stable with respect to the increment of the basis set with higher-n Rydberg orbitals.

In conclusion, we have demonstrated that one-step calculations allow us to predict the main features of the interference effects observed in measurements. The one-step approximation used in the calculations was found to be able to qualitatively explain the detected resonant enhancement of the $4p^4nl$ states, especially of the $4p^4(^1D)4d(^2S_{1/2})$ line, when the photon energy was tuned through the $3d^94p^5nln'l'$ resonances.

ACKNOWLEDGMENTS

The staff of MAX laboratory is acknowledged for assistance during the measurements. This work was supported by the Research Council for the Natural Sciences of the Academy of Finland and EU TMR Program under Contract No. ERB FMGE CT98 0124.

[1] G. B. Armen, H. Aksela, T. Åberg, and S. Aksela, J. Phys. B **32**, R1 (1999).
[2] O.-P. Sairanen, A. Kivimäki, E. Nõmmiste, H. Aksela, and S. Aksela, Phys. Rev. A **54**, 2834 (1996).
[3] N. Berrah, B. Langer, J. Bozek, T. W. Gorczyca, O. Hemmers, D. W. Lindle, and O. Toader, J. Phys. B **29**, 5351 (1996).
[4] J. M. Bizau and F. J. Wuilleumier, J. Electron Spectrosc. Relat. Phenom. **71**, 205 (1995).
[5] A. Menzel, S. P. Frigo, S. B. Whitfield, and C. D. Caldwell, Phys. Rev. A **54**, 2080 (1996).
[6] J. Tulkki, S. Aksela, H. Aksela, E. Shigemasa, A. Yagishita, and Y. Furusawa, Phys. Rev. A **45**, 4640 (1992).
[7] A. Ehresmann, F. Vollweiler, H. Schmoranzer, V. L. Sukhorukov, B. M. Lagutin, I. D. Petrov, G. Mentzel, and K.-H. Schartner, J. Phys. B **27**, 1489 (1994).
[8] E. Murakami, T. Hayaishi, A. Yagishita, and Y. Morioka, Phys. Scr. **41**, 468 (1990).
[9] J. A. R. Samson, W. C. Stolte, Z.-X. He, J. N. Cutler, and Y. Lu, Phys. Rev. A **57**, 1906 (1998).
[10] R. I. Hall, A. McConkey, K. Ellis, G. Dawber, M. A. MacDonald, and G. C. King, J. Phys. B **25**, 799 (1992).
[11] B. Rouvellou, L. Journel, J. M. Bizau, D. Cubaynes, F. J. Wuilleumier, M. Richter, K.-H. Selbmann, P. Sladeczek, and P. Zimmermann, Phys. Rev. A **50**, 4868 (1994).
[12] K. Maier, A. Kivimäki, B. Kempgens, U. Hergenhahn, M. Neeb, A. Rüdel, M. N. Piancastelli, and A. M. Bradshaw, Phys. Rev. A **58**, 3654 (1998).
[13] C. Reynaud, M.-A. Gaveau, K. Bisson, P. Millié, I. Nenner, S. Bodeur, P. Archirel, and B. Lévy, J. Phys. B **29**, 5403 (1996).
[14] H. Aksela, S. Alitalo, J. Jauhiainen, A. Kivimäki, T. Matila, T. Kylli, E. Nõmmiste, and S. Aksela, Phys. Rev. A **59**, R2563 (1999).
[15] J. A. R. Samson, Y. Chung, and E. M. Lee, Phys. Rev. A **45**, 259 (1992).
[16] T. Hayaishi, E. Murakami, Y. Morioka, H. Aksela, S. Aksela, E. Shigemasa, and A. Yagishita, Phys. Rev. A **44**, R2771 (1991).
[17] H. Aksela, S. Aksela, O.-P. Sairanen, A. Kivimäki, A. Naves de Brito, E. Nõmmiste, J. Tulkki, S. Svensson, A. Ausmees, and S. J. Osborne, Phys. Rev. A **49**, R4269 (1994); H. Aksela, O.-P. Sairanen, S. Aksela, A. Kivimäki, A. Naves de Brito, E. Nõmmiste, J. Tulkki, A. Ausmees, S. J. Osborne, and S. Svensson, *ibid.* **51**, 1291 (1995).
[18] A. Kikas, S. J. Osborne, A. Ausmees, S. Svensson, O.-P. Sairanen, and S. Aksela, J. Electron Spectrosc. Relat. Phenom. **77**, 241 (1996).
[19] R. D. Cowan, *The Theory of Atomic Structure and Spectra* (University of Califoria Press, Berkeley, 1981).
[20] R. D. Cowan and D. C. Griffin, J. Opt. Soc. Am. **66**, 1010 (1976).
[21] M. Blume and R. E. Watson, Proc. R. Soc. London, Ser. A **270**, 127 (1962); M. Blume and R. E. Watson, *ibid.* **271**, 565 (1963).
[22] R. Nyholm, S. Svensson, J. Nordgren, and A. Flodström, Nucl. Instrum. Methods Phys. Res. A **246**, 267 (1986); S. Aksela, A. Kivimäki, R. Nyholm, and S. Svensson, Rev. Sci. Instrum. **63**, 1252 (1992).
[23] N. Mårtensson, P. Baltzer, P. A. Brühwiler, J.-O. Forsell, A. Nilsson, A. Stenborg, and B. Wannberg, J. Electron Spectrosc. Relat. Phenom. **70**, 170 (1994).
[24] L. Minnhagen, H. Strihed, and B. Petersson, Ark. Fys. **39**, 471 (1968).
[25] *Atomic Energy Levels*, edited by C. E. Moore, Natl. Bur. Stand. U.S. Circ. No 467 (U.S. GPO, Washington, DC, 1952), Vol. II.